

EFFECT OF A MAGNETIC FIELD ON THE MICROSTRUCTURE AND PROPERTIES OF RESISTANCE SPOT WELDED JOINTS OF 444 FERRITIC STAINLESS STEEL/6082 ALUMINUM ALLOY

VPLIV MAGNETNEGA POLJA NA MIKROSTRUKTURU IN LASTNOSTI UPOROVNO TOČKOVNO ZVARJENEGA FERITNEGA NERJAVNEGA JEKLA TIP 444 IN Al ZLITINE TIP 6082

Xiaouo Zhu^{1*}, Zhanqi Liu¹, Qi Zhou¹, Jie Chen², Shouhong Li²

¹School of Materials Science and Engineering, Liaoning University of Technology, Jinzhou, China

²Panasonic Welding Systems (Tangshan) Co., Ltd., China

Prejem rokopisa – received: 2023-11-27; sprejem za objavo – accepted for publication: 2024-01-22

doi:10.17222/mit.2023.1055

To improve the welding quality of resistance spot welding joints of steel/aluminum lightweight structures, the steady magnetic field-assisted resistance spot welding method was used to weld 444 ferritic stainless steel and 6082 aluminum alloy, both with a thickness of 1 mm. Under the same welding parameters, the effect of a magnetic field on the microstructure and mechanical properties of the joint was analyzed. It was found that the Lorentz force generated by the addition of a magnetic field promoted the circumferential movement of the molten metal in the nugget zone, increased the size of the Fe/Al contact interface in the joint along the horizontal direction, and made an effective use of the heat generated during resistance spot welding. Although the intermetallic compounds in the intermediate transition layer of the two welded materials were mainly composed of (Fe, Cr, Si)Al₂ and (Fe, Cr, Si)Al₃, relatively low contents of (Fe, Cr, Si)Al₂ and (Fe, Cr, Si)Al₃ were found and there was a significant decrease in the thickness of the intermetallic compound layer when the magnetic field was applied. Compared with the welded joint devoid of a magnetic field, the tensile strength and ductility of the joint were effectively improved, and the dimples in the fracture surface became relatively deep and numerous. In essence, resistance spot welding joints of steel/aluminum obtain better comprehensive mechanical properties when a magnetic field is applied.

Keywords: stainless steel, aluminum alloy, magnetic field-assisted resistance spot welding, mechanical properties

Avtorji članka so zato, da bi izboljšali kvaliteto uporovno točkovno zvarjenih spojev lahkih konstrukcij sestavljenih iz nerjavnega jekla in aluminijevih zlitin uporabili postopek uporovnega točkovnega varjenja podprtega s stalnim magnetnim poljem. Za preizkuse varjenja so uporabili preizkušance iz pločevine feritnega nerjavnega jekla vrste 444 in Al zlitine vrste 6082 debeline 1 mm. Pri enakih parametrih varjenja so določili vpliv spremembe gostote magnetnega polja na mikrostrukturo in mehanske lastnosti zvarnih spojev. Ugotovili so da Lorentzova sila povzročena z magnetni poljem pospešuje gibanje robov raztaljene kovine proti središču zvarnih spojev, kar povečuje velikost kontaktne površine med Fe in Al v spoju vzdolž vodoravne smeri in s tem poveča izkoristek toplote nastale med varjenjem. Čeprav je bila vmesna prehodna cona zvara v glavnem sestavljena iz intermetalnih spojin (Fe, Cr, Si)Al₂ in (Fe, Cr, Si)Al₃, se je debelina sloja iz teh intermetalnih spojin pomembno zmanjšala v prisotnosti magnetnega polja. Natezna trdnost in duktilnost zvarnih spojev se je učinkovito izboljšala zaradi prisotnosti stalnega magnetnega polja ter prelomna površina zvarov je postala jamičasto duktilna. V bistvu uporovno točkovno varjenje nerjavnega jekla in aluminija, podprto s stalnim magnetnim poljem celovito izboljša mehanske lastnosti zvarnih spojev te vrste.

Ključne besede: nerjavno jeklo, zlitina na osnovi aluminija, z magnetnim poljem podprto uporovno točkovno varjenje, mehanske lastnosti

1 INTRODUCTION

With the increasing pursuit of low-energy consumption in the manufacturing industry, hybrid structures composed of stainless steel and an aluminum alloy are increasingly used for automobiles, spacecraft and ships to obtain high rigidity and lightweight structures.¹ At present, the biggest problem of combining dissimilar metals, i.e., aluminum and steel is the formation of an Al-Fe brittle intermetallic compound (hereinafter referred to as IMC).^{1,2}

As the base metal remains solid during resistance spot welding (henceforth referred to as RSW) and the welding temperature is low, the interatomic interaction

and diffusion at the interface are substantially diminished. Consequently, the generation of the IMC can be suppressed to a great extent, enabling a high-quality connection of Fe/Al dissimilar metals, which is an effective way from a theoretical point of view.^{2,3}

Simultaneously, a number of scholars have conducted in-depth research on the RSW of stainless steel and aluminum alloy.⁴⁻⁶ Despite the fact that currently an aluminum alloy and stainless steel can be connected by RSW, the physical and chemical properties of Al and Fe are quite different, and their solid solubility is negligible. Therefore, a substantial IMC persists in an Al/Fe joint formed by RSW, affecting the improvement of the joint's tensile properties. When the thickness of the IMC exceeds 1.5 μm , the mechanical properties of the joint are found to deteriorate seriously.^{5,6}

*Corresponding author's e-mail:
clzxo@lnut.edu.cn (Xiaouo Zhu)

Experimental investigations confirmed that, unlike arc welding and laser welding, RSW does not need to be filled with a welding wire, the molten pool solidifies rapidly due to a short welding period, and the resulting weld is often prone to shrinkage defects.⁷

Presently, researchers have found that the application of a magnetic field into the welding process can effectively improve the mechanical properties of welded joints, representing a feasible auxiliary welding method. Although there is no obvious arc or liquid molten pool in RSW, the presence of the current ensures that the magnetic field continues to have an important role. Some scholars that apply a magnetic field to the RSW of Fe/Al dissimilar metals discover that it greatly improves the mechanical properties of the joint.^{8,9}

Ferrite stainless steel and a 6XXX aluminum alloy are widely used in the automobile industry, marine engineering and other fields because of their exceptional weldability and unique advantages.^{10,11} Therefore, the connecting of the two materials is both necessary and possible. However, at present, an analysis of the microstructure and properties of dissimilar-metal RSW joints between the above two materials is limited, as is research on the effect of the microstructure and properties of welded joints that occur after an external magnetic field is applied.

In this paper, 444 ferritic stainless steel (henceforth referred to as 444) and 6082 aluminum alloy (hereinafter referred to as 6082) are taken as the research objects, and a steady-state magnetic field is applied during the resistance spot welding test (MA-RSW) of Fe/Al dissimilar

materials to explore the influence of the steady-state magnetic field on the macro-morphology, microstructure and tensile properties of Fe/Al welded joints, so as to optimize the welding process parameters of Fe/Al dissimilar materials and broaden the application range of magnetic field-assisted welding.

2 EXPERIMENTAL PART

The materials selected for this experiment included 444 and 6082, both of which were manufactured in China, with corresponding supply statuses of cold-rolled and T6. The sample dimensions of the two materials were (75 × 20 × 1) mm. The alloy elements and mechanical properties of the two materials are shown in **Tables 1** and **2**, respectively.

Table 1: Alloy elements' maximum concentrations (wt.%)

	C	Si	Mn	Cr	P	S	Mg	Al	Fe
444	0.025	1.0	1.0	18.0	0.035	0.03	–	–	Bal.
6082	–	1.3	0.95	0.25	–	–	1.1	Bal.	0.5

Table 2: Mechanical properties (minimum)

	Yield strength (MPa)	Tensile strength (MPa)
444	245	410
6082	260	310

Initially, the RSW samples were overlapped up and down along the horizontal direction, with an overlapping area of (20 × 20) mm, the top of which was 6082 and the bottom was 444. An RSW test was conducted at the cen-

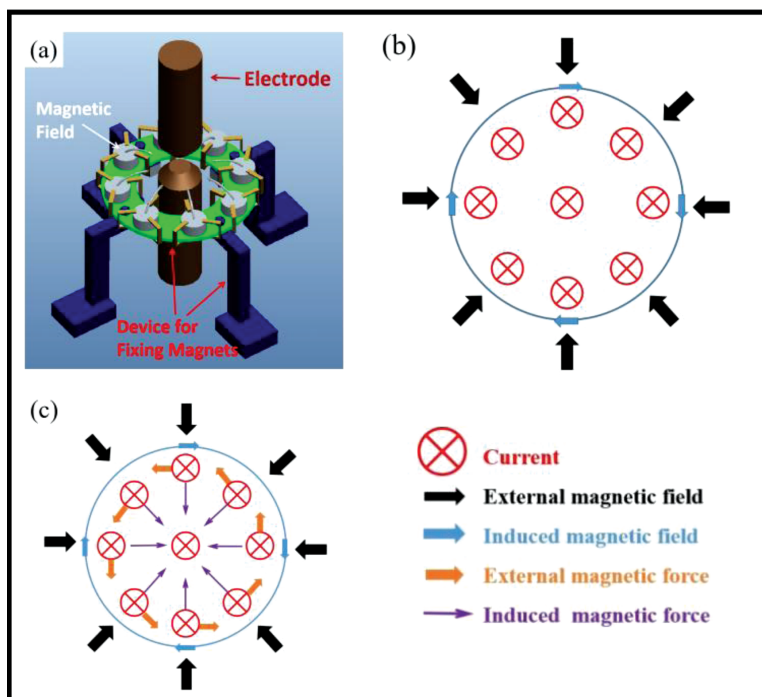


Figure 1: Schematic diagram of welding technology: a) MA-RSW apparatus, b) magnetic field distribution at the faying surface, c) magnetic force at the faying surface

ter of the lap joint using a Panasonic YR-350 S single-phase AC resistance welder. The electrode material was Cr-Zr-Cu, with a 5-mm-diameter end face and an electrode pressure of 2.0 kN; the welding time was 20 cycles, and three groups of RSW tests were carried out with a welding current of 10.5 kA.

In order to explore the effect of a magnetic field on the microstructure and mechanical properties of RSW welded joints, three sets of MA-RSW experiments were carried out. After adopting the same pre-welding preparation and welding process parameters, eight NdFeB cylindrical permanent magnets, each measuring 6 mm in diameter and 3 mm in thickness, were horizontally affixed around the electrode while maintaining a surface magnetic induction of 30 mT. The arrangement of the magnets is as shown in **Figure 1a**, and the magnetic induction lines produced by the permanent magnets pass through the welding nugget to form the Lorentz force. **Figure 1b** illustrates the directions of the induced magnetic field and the external magnetic field.^{8,9} In this structure, the interaction between the external magnetic field and welding current produces a circumferential Lorentz force, which promotes the circumferential movement of the molten metal inside the nugget,^{8,9} as shown in **Figure 1c**. Under the combined influence of the induced magnetic field and the external magnetic field,¹² the Lorentz force monotonically grows from the center of the nugget to its edge, propelling the molten metal in all directions from the welding center.¹³

To reveal the microstructure of the interface area, a metallographic sample of the joint was prepared using wire cutting after the welding, followed by polishing and etching with the Keller reagent, 5 mL nitric acid, 1 mL HF and 44 mL water. The macro-morphology of the joint was observed using a Zeiss Stemi 508 stereoscopic microscope, while the nugget size and the fracture area were recorded. Using a Zeiss SIGMA 300 field-emission

scanning electron microscope (SEM), an energy dispersive spectrometer (EDS) and an Ultima IV combined multifunctional horizontal X-ray diffractometer (XRD), the structure and characteristics of the IMC at the Fe/Al interface of two welded joints were observed. Six groups of welded joints were measured utilizing a CMT 5305 electronic universal testing machine, and the value of the peak load of each group was documented. In order to ensure the stress uniformity during the tensile test, $1 \times 20 \times 20$ mm steel plates were positioned on the surfaces of both extremities of a sample. The fracture morphology was observed using SEM.

3 RESULTS AND DISCUSSION

It is evident from **Figures 2a** and **2b** that the structures of the RSW and MA-RSW joints include two nuggets, one in the 444 plate and the other in the 6082 plate; there are no welding defects such as shrinkage, and the weld is well-formed. The 444 plates within the two welded joints solidified to form nuggets that were oval; the nuggets of 6082 solidified in the direction of the Fe/Al surface toward the interior of the 6082 plates, showing a trapezoidal shape. Through measurement and comparison, it is observed that the nugget sizes for the two welded joints are obviously different. In the RSW joint, the nugget diameter of 444 is 4.6 mm, and in the MA-RSW joint, the nugget diameter of 444 is higher by 6.6 %, that is, 4.9 mm. In the RSW joint, the upper width of the 6082 nugget is 5.0 mm, while the lower width is 2.95 mm; In the MA-RSW joint, the upper width is higher by 10 %, that is, 5.5 mm, and the lower width is decreased by 18.64 %, that is, 2.4 mm. The corner of the 6082 block in the RSW joint is about 140° , while in the MA-RSW joint, it is about 155° , representing an increase of 10.71 %.

This is due to the fact that during the conventional RSW of Fe/Al, 75 % of heat is concentrated in the Fe plate used for heating the Al plate, resulting in the formation of Al side and 444 inside nuggets.¹⁴ During MA-RSW, the Lorentz force generated by the external magnetic field accelerates the circumferential movement of the 444 molten metal towards the outside of the nugget, hence causing the nugget to grow in size. Simultaneously, the Lorentz force also extends the upper part of the 6082 nuggets outward on the Fe/Al surface along the horizontal line, leading to a reduction in the heat transfer to the interior of the Al plate, causing the corner of the upper width of the Al side nugget to increase and the length of the lower width to decrease significantly. After the addition of the magnetic field, the contact surface area of Fe/Al increases and the heat of RSW is effectively utilized.

Figure 3 shows the SEM microstructure and EDS analysis of the IMC at the Fe/Al interface in the center of the weld. As can be seen from **Figure 3**, the thickness of the IMC at the center of the RSW joint is $2.6 \mu\text{m}$, while

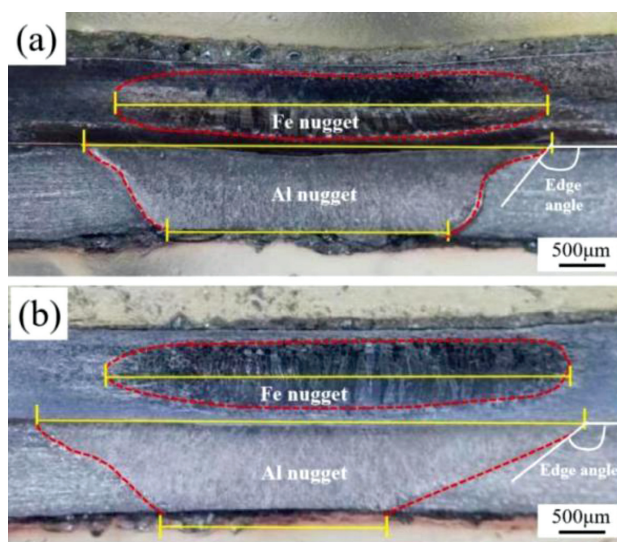


Figure 2: Macro-morphology of cross-sections: a) RSW, b) MA-RSW

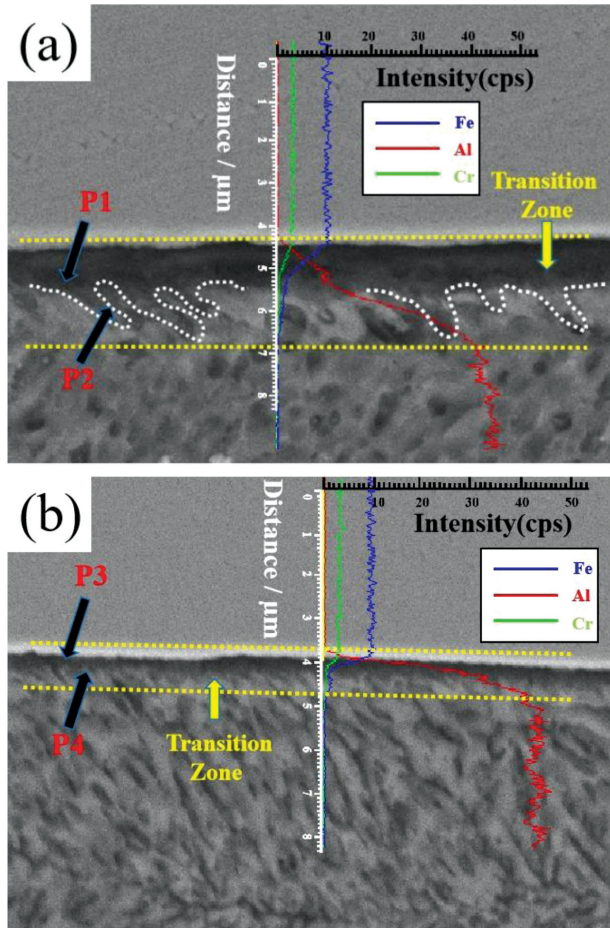


Figure 3: IMC layer characteristics: a) RSW, b) MA-RSW

it is 1.0 μm at the center of the MA -RSW joint, indicating a 61.54 % reduction.

The obtained result can be explained using the reaction diffusion principle, that is, the thickness X of the interfacial reaction layer can be expressed as Equation 1¹⁵:

$$X = \left[2k_0 \exp\left(-\frac{Q}{RT}\right) \right]^{1/2} \quad (1)$$

where k_0 is the growth constant of the reaction layer, Q denotes the activation energy of the growth of the reaction layer, R is the gas constant, T represents the heating temperature, and t is the reaction time.

According to Equation (1), X is related to t , that is, as the heating temperature increases, so does the reaction time, and the thickness of the reaction layer is increased. In the process of MA-RSW, the Lorentz force promotes

the circular motion of the molten metal, leading to a relatively low maximum temperature in the central area of the joint interface and rapid heat dissipation, which in turn shortens the reaction time and reduces the thickness of the interface reaction layer to a certain extent. Meanwhile, according to references,^{15,16} it can be inferred that the reaction layer is thicker in the central area and decreases with an increasing distance from the weld center. A reduction in the IMC thickness reduces the crack sensitivity and improves ductility.¹⁷

In the center of the RSW weld, only the flat surface of the 444 side and the serrated surface of the 6082 side are observed at the interface, which aligns well with the results observed in reference.¹⁵ However, the IMC thickness is considerably reduced in the center of the MA-RSW weld, resulting in a flat surface on the two sides of the Fe/Al interface, as shown in Figure 3.

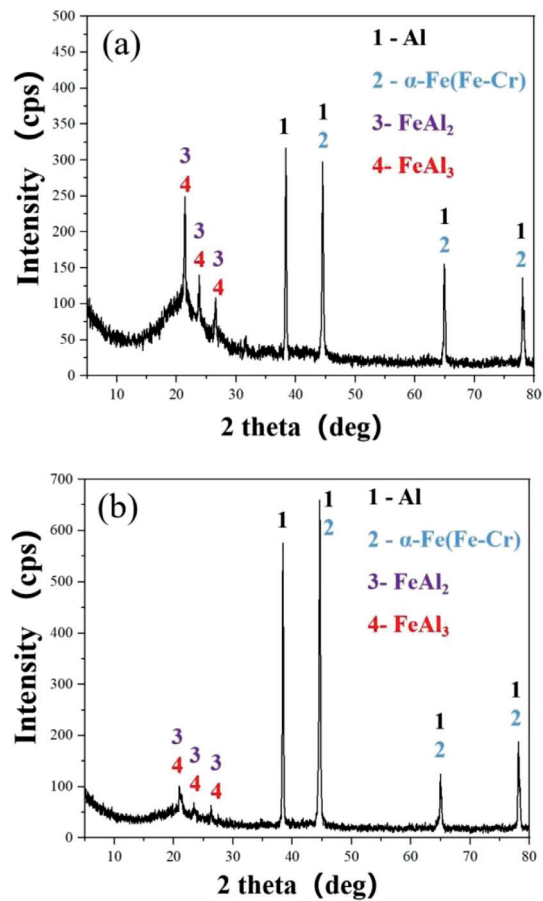


Figure 4: Micro-X-ray diffraction curve: a) RSW, b) MA-RSW

Table 3: EDS analysis results for the IMC layer

Elements	Al		Fe		Cr		Possible compound composition
	wl%	ϕl%	wl%	ϕl%	wl%	ϕl%	
P1	68.25	81.46	26.30	15.17	5.45	3.38	Al, α-Fe-Cr (a small amount), FeAl ₂ and FeAl ₃
P2	82.74	90.71	13.64	7.22	3.63	2.06	
P3	0.43	0.88	81.64	80.20	17.93	18.91	
P4	60.71	75.96	32.89	19.88	5.39	3.31	

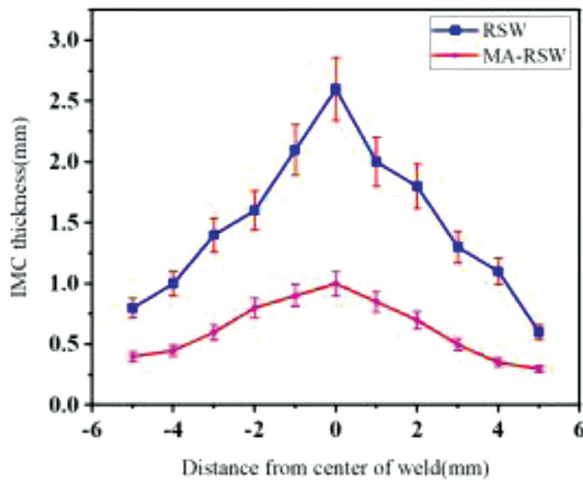


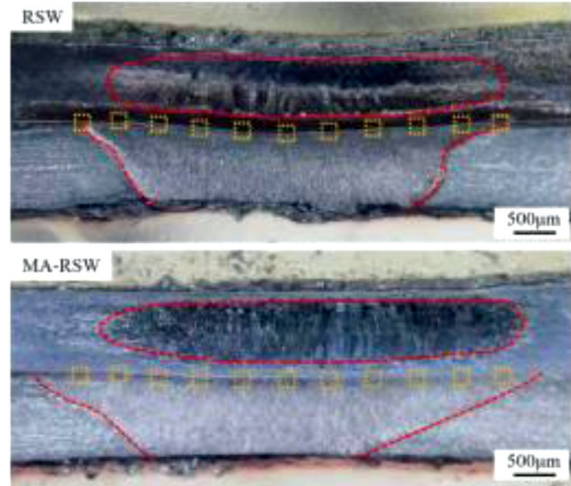
Figure 5: IMC thickness statistics of RSW and MA-RSW welds

Figures 3a and 3b also show the findings of the linear scanning analysis of EDS perpendicular to the Fe/Al interface, demonstrating that Al and Fe have undergone mutual diffusion. At the same time, it is found that the Lorentz force increases the diffusion of Fe into the transition zone and reduces the Al proportion in the IMC region, which is consistent with the results of the EDS point scanning analysis of the IMC layer presented in Table 3.

Combined with the XRD and EDS data shown in Figure 4 and Table 3, respectively, it is confirmed that the primary components of the IMC at the Fe/Al interface are FeAl₂ and FeAl₃ prior to the addition of the magnetic field. Due to the presence of trace amounts of Cr and Si that are unavoidable, the phase composition of the components indicated in Figure 4a can be expressed as iron-rich (Fe, Cr, Si)Al₂ (FeAl₂) and aluminum-rich (Fe, Cr, Si)Al₃ (FeAl₃). A similar finding was also found by Ranfeng et al.^{17,18}

During MA-RSW, the electromotive force facilitates the acceleration of Fe diffusion within the melting zone, reduces the maximum interface temperature, shortens the dwell time at high-temperatures, and inhibits the nucleation of FeAl₂ and FeAl₃, consequently reducing the thickness of the IMC layer and undoubtedly improving the plasticity of the welded joint structure.¹⁹ In contrast to Figure 4a, Figure 4b illustrates a comparatively reduced composition of FeAl₂ and FeAl₃, a finding that corroborates the aforementioned analysis.

For the two types of welds, SEM was used to determine the IMC thickness of 11 evenly distributed areas at the Fe/Al interface; the corresponding statistical results are shown in Figure 5. Statistics show that the IMC thickness in the center near the Fe/Al interface in the RSW welds is maximum, measuring 2.6 μm, and it is minimum in the outermost position, measuring 0.6 μm. In the MA-RSW welds, the maximum IMC thickness is observed at the center near the Fe/Al interface, measuring 1.0 μm, while the minimum is observed at the weld's



edge, measuring 0.3 μm. The result shown in Figure 5 is consistent with the analysis and assumption based on Equation 1 and references.^{15,16} It is thus anticipated that an MA-RSW welded joint with a thin IMC layer would exhibit excellent tensile properties.

Figure 6 shows the load-extension curves of RSW and MA-RSW joints. Comparatively speaking, it is not difficult to conclude that MA-RSW joints can obtain a greater ductility. Three groups of RSW tensile samples have an average peak load of 1786.67 N, whereas the average peak load of three groups of MA-RSW tensile samples is 3613.33 N, which is 102.2 % higher than that of RSW tensile samples. This result is attributed to the increase in the Fe/Al horizontal contact interface area of the joint due to the Lorentz force generated after the addition of the magnetic field. In addition, the thickness of the IMC at the interface is substantially reduced, which also plays an important role in enhancing the tensile properties of the joint.

Fracture morphologies of RSW and MA-RSW joints on the Al plate are illustrated in Figure 7. As determined with a stereoscopic microscope, the dark gray region situated at the center of the two welds is the fracture area.

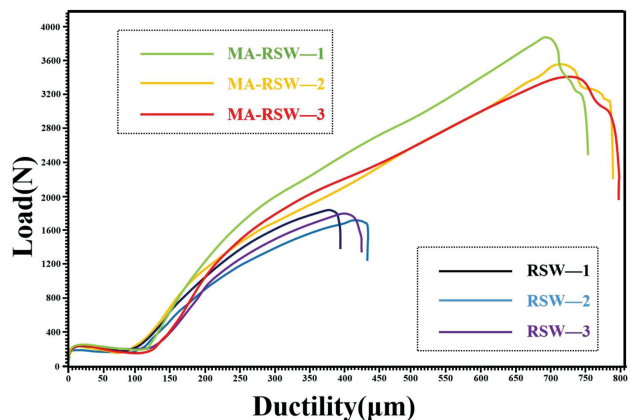


Figure 6: Load-ductility curves of welded joints

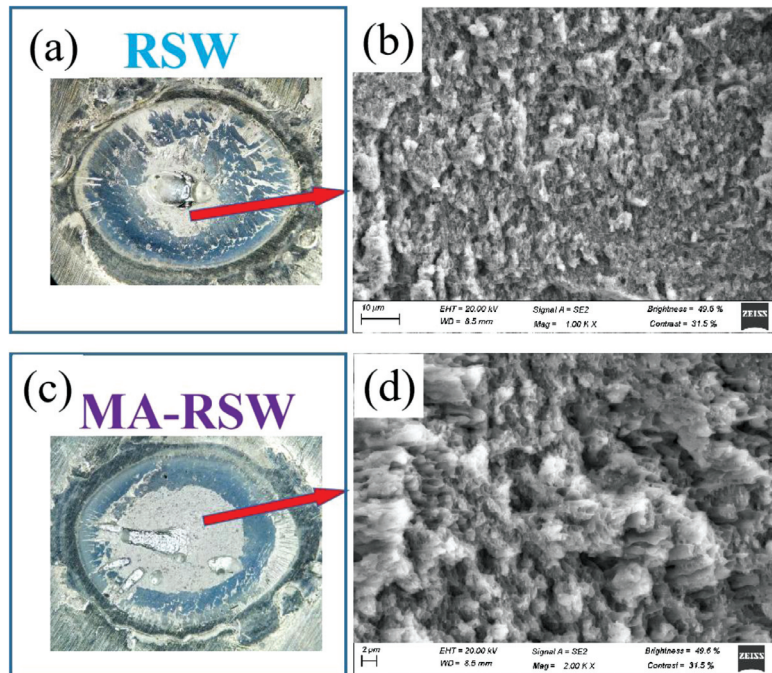


Figure 7: Fracture morphology

Based on the SEM observation, we can see that the fracture surfaces of these two joints are mostly brittle. Among them, the dimple on the fracture surface of the RSW joint is relatively shallow and the fracture area is relatively small, significantly diminishing the mechanical properties of the joint. On the other hand, the fracture dimple of the MA-RSW joint is comparatively deep as a result of a substantial drop in the IMC thickness and component content, so the plasticity of the joint is dramatically improved. This is consistent with the analysis results shown in **Figures 5 and 6**.

4 CONCLUSIONS

The 444-6082 welded joints devoid of obvious welding defects were obtained with both RSW and MA-RSW, and the joint structures exhibited two nuggets, located in 444 and 6082. However, the external magnetic field caused a 6.6 % rise in the size of the nugget on 444, a 10 % increase in the upper width, a 10.71 % increase in the corner of the 6082 block, and an 18.64 % drop in the lower width. The contact surface area of Fe/Al increased. This finding demonstrates that the addition of a magnetic field significantly improves the heat-utilization efficiency of RSW.

The IMC transition layers of the two joints predominantly consist of $(\text{Fe, Cr, Si})\text{Al}_2$ and $(\text{Fe, Cr, Si})\text{Al}_3$. The IMC has a greater thickness in the central region and a diminishing thickness with an increasing distance from the center of the 444-6082 joints. The introduction of a magnetic field induces the Lorentz force, which expedites the diffusion of Fe within the melting zone, reduces the high-temperature dwell time of the transition layers,

prevents the nucleation of internal IMC, and results in a relatively reduced content of IMC, while the peak thickness of internal IMC decreases by 61.54 %.

Under the action of the external magnetic field, the average peak load of MA-RSW joints is 3613.33 N, which is 102.2 % higher than that of RSW joints. At the same time, the fracture dimples of these joints are deeper and larger, and the comprehensive mechanical properties are improved.

Acknowledgment

The authors would like to acknowledge the support from the Basic Scientific Research Project of Liaoning Provincial Department of Education (grant number: JYTMS20230848), and the Doctoral Start-up Foundation of Liaoning Province (grant number: 2023-BS-195).

5 REFERENCES

- ¹ M. A. Ezazi, F. Yusof, A. Sarhan, et al., Employment of fiber laser technology to weld austenitic stainless steel 3041 with aluminum alloy 5083 using pre-placed activating flux, *Mater. Des.*, 87 (2015), 105–123, doi:10.1016/j.matdes.2015.08.014
- ² A. K. Deepati, W. Alhazmi, I. Benjeer, Mechanical characterization of AA5083 aluminum alloy welded using resistance spot welding for the lightweight automobile body fabrication, *Materials Today: Proceedings*, 45 (2021), 5139–5148, doi:10.1016/j.matpr.2021.01.646
- ³ Y. Ogawa, I. Ohara, J. Arakawa, H. Akebono, A. Sugeta, Effects of welding defects on the fatigue properties of spot welded automobile steel sheets and the establishment of a fatigue life evaluation method, *Welding in the World*, 66 (2022), 745–752, doi:10.1007/s40194-021-01238-5
- ⁴ R. Qiu, C. Iwamoto, S. Satonaka, The influence of reaction layer on the strength of aluminum/steel joint welded by resistance spot weld-

- ing, *Materials Characterization*, 60 (2009), 156–159, doi:10.1016/j.matchar.2008.07.005
- ⁵ A. S. Baskoro, H. Muzakki, G. Kiswanto, et al., Mechanical Properties and Microstructures on Dissimilar Metal Joints of Stainless Steel 301 and Aluminum Alloy 1100 by Micro-Resistance Spot Welding, *Transactions of the Indian Institute of Metals*, Springer India, 72 (2019), 487–500, doi:10.1007/s12666-018-1500-z
- ⁶ H. Muzakki, A. S. Baskoro, G. Kiswanto, W. Winarto, Mechanical Properties of the Micro Resistance Spot Welding of Aluminum Alloy to Stainless Steel with a Zinc Interlayer, *International Journal of Technology*, 9 (2018), 686–694, doi:10.14716/ijtech.v9i4.1867
- ⁷ N. Sridharan, J. Poplawsky, A. Vivek, et al., Cascading microstructures in aluminum-steel interfaces created by impact welding, *Materials Characterization*, 151 (2019), 119–128, doi:10.1016/j.matchar.2019.02.019
- ⁸ Y. B. Li, Q. X. Zhang, L. Qi, et al., Improving austenitic stainless steel resistance spot weld quality using external magnetic field, *Science and Technology of Welding and Joining*, 23 (2018), 619–627, doi:10.1080/13621718.2018.1443997
- ⁹ L. Qi, F. Li, R. Chen, et al., Improve resistance spot weld quality of advanced high strength steels using bilateral external magnetic field, *Journal of Manufacturing Processes*, 52 (2020), 270–280, doi:10.1016/j.jmapro.2020.02.030
- ¹⁰ J. Zhou, J. Shen, S. Hu, et al., Microstructure and mechanical properties of AISI 430 ferritic stainless steel joints fabricated by cold metal transfer welding, *Materials Research Express*, 6 (2019), 116536, doi:10.1088/2053-1591/ab4770
- ¹¹ Z. Xin, Z. Yang, H. Zhao, et al., Comparative Study on Welding Characteristics of Laser-CMT and Plasma-CMT Hybrid Welded AA6082-T6 Aluminum Alloy Butt Joints, *Materials*, 12 (2019), 3300, doi:10.3390/ma12203300
- ¹² Y. B. Li, Z. Q. Lin, X. M. Lai, et al., Induced electromagnetic stirring behavior in a resistance spot weld nugget, *Sci. China Technol. Sci.*, 53 (2010), 1271–1277, doi:10.1007/s11431-010-0086-4
- ¹³ Y. B. Li, D. L. Li, S. A. David, et al., Microstructures of magnetically assisted dual-phase steel resistance spot welds, *Science and Technology of Welding and Joining*, 21 (2016), 555–563, doi:10.1080/13621718.2016.1141493
- ¹⁴ Z. Wan, H. Wang, M. Wang, et al., Numerical simulation of resistance spot welding of Al to zinc-coated steel with improved representation of contact interactions, *Int. J. Heat Mass Tran.*, 101 (2016), 749–763, doi:10.1016/j.ijheatmasstransfer.2016.05.023
- ¹⁵ Y. Zhang, D. Sun, Microstructures and Mechanical Properties of Steel/Aluminum Alloy Joints Welded by Resistance Spot Welding, *Journal of Materials Engineering & Performance*, 26 (2017), 2649–2662, doi:10.1007/s11665-017-2731-6
- ¹⁶ Q. Shen, Y. B. Li, Z. Q. Lin, et al., Effect of external constant magnetic field on weld nugget of resistance spot welded dual-phase steel DP590, *IEEE Transactions on Magnetics*, 47 (2011), 4116–4119, doi:10.1109/tmag.2011.2157316
- ¹⁷ J. Sun, Q. Yan, W. Gao, J. Huang, Investigation of laser welding on butt joints of Al/steel dissimilar materials, *Materials and Design*, 83 (2015), 120–128, doi:10.1016/j.matdes.2015.05.069
- ¹⁸ R. Qiu, C. Iwamoto, S. Satonaka, Interfacial Microstructure and Strength of Steel/Al Alloy Joints Welded by RSW with Cover Plate, *J. Mater. Process. Technol.*, 209 (2009), 4186–4193, doi:10.1016/j.jmatprotec.2008.11.003
- ¹⁹ D. Sun, Y. Zhang, Y. Liu, et al., Microstructures and mechanical properties of resistance spot welded joints of 16Mn steel and 6063-T6 aluminum alloy with different electrodes, *Materials & Design*, 109 (2016), 596–608, doi:10.1016/j.matdes.2016.07.076